Molecular Therapy
Nucleic Acids
Original Article

Long Non-coding RNA JHDM1D-AS1 Interacts with DHX15 Protein to Enhance Non-Small-Cell Lung Cancer Growth and Metastasis

Guodong Yao,[1] Kexin Chen,[1] Yu Qin,[1] Yangyang Niu,[1] Xuefang Zhang,[1] Shidong Xu,[2] Chi Zhang,[3] Meiyan Feng,[1] and Kuan Wang[4]

[1]Department of Pathology, Harbin Medical University Cancer Hospital, Harbin, China; [2]Department of Thoracic Surgery, Harbin Medical University Cancer Hospital, Harbin, China; [3]Brandeis University, Waltham, MA, USA; [4]Department of Gastrointestinal Surgery, Harbin Medical University Cancer Hospital, Harbin, China

JHDM1D antisense 1 (JHDM1D-AS1), a long non-coding RNA (lncRNA), has been shown to promote pancreatic cancer growth by inducing an angiogenic response. However, its biological and clinical significance in non-small-cell lung cancer (NSCLC) is still unclear. In this study, we examined the expression and prognostic significance of JHDM1D-AS1 in NSCLC. The effects of JHDM1D-AS1 knockdown or overexpression on NSCLC growth and metastasis were investigated. We show that JHDM1D-AS1 is upregulated in NSCLC relative to adjacent normal lung tissues. High JHDM1D-AS1 expression is significantly correlated with advanced tumor, node, and metastasis (TNM) stage and lymph node metastasis. JHDM1D-AS1 expression serves as an independent prognostic factor for overall survival of patients with NSCLC. Functionally, JHDM1D-AS1 knockdown inhibits NSCLC cell aggressiveness both *in vitro* and *in vivo*, which is rescued by ectopic expression of JHDM1D-AS1. JHDM1D-AS1 binding stabilizes DHX15 protein in NSCLC cells. DHX15 overexpression enhances NSCLC cell proliferation and invasion, whereas knockdown of DHX15 exerts opposite effects. JHDM1D-AS1-mediated aggressive phenotype is impaired when DHX15 is silenced. Ectopic expression of DHX15 restores the defects in proliferation and invasion of JHDM1D-AS1-depleted NSCLC cells. Collectively, the interaction between JHDM1D-AS1 and DHX15 accounts for NSCLC growth and metastasis. This work provides potential additional therapeutic targets for treatment of NSCLC.

INTRODUCTION

Lung cancer is one of the most common malignancies and the leading cause of cancer-related death worldwide.[1,2] Non-small-cell lung cancer (NSCLC) accounts for about 85% of all lung cancers.[3] The predicted 5-year survival rate for NSCLC is as low as 15.9%.[3] The poor prognosis of NSCLC is largely ascribed to development of metastatic disease. Identification of the molecular mechanisms for cancer metastasis is of significance in developing effective therapeutic approaches for NSCLC.

DHX15 is a member of the DEXD/H box helicase family that participates in ATP-dependent unwinding of RNA substrates, consequently modulating pre-mRNA splicing and translation initiation.[4,5] DHX15 has been shown to recognize viral RNA and activate immune response through nuclear factor κB (NF-κB) and mitogen-activated protein kinase (MAPK) signaling in myeloid dendritic cells.[6] Memet et al.[7] reported that DHX15 is involved in ribosome biogenesis by promoting pre-rRNA cleavage.[7] DHX15 has been documented to modulate gene expression by repressing CMTR1-dependent mRNA cap formation.[8] Recent reports have indicated the role of DHX15 in cancer progression.[9–11] For instance, Ito et al.[9] reported that DHX15 is downregulated in glioma, and overexpression of DHX15 suppresses glioma growth both *in vitro* and *in vivo*. Jing et al.[10] demonstrated that DHX15 acts as a co-activator of androgen receptor (AR) and promotes prostate cancer progression by enhancing AR transcriptional activity. DHX15 is upregulated and shows a significant correlation with poor prognosis in hepatocellular carcinoma.[11] These studies suggest that DHX15 plays a context-specific role in cancer progression.

Long non-coding RNAs (lncRNAs) are a class of regulatory non-coding RNA molecules of >200 nt in length.[12] They are frequently dysregulated in cancer and modulate multiple aspects of tumor biology.[13–15] For instance, the lncRNA PVT1 is upregulated in NSCLC and promotes cancer cell proliferation, invasion, and radioresistance.[14] Xu et al.[15] reported that the lncRNA Linc-GALH accelerates hepatocellular carcinoma metastasis. JHDM1D antisense 1 (JHDM1D-AS1) is a nutrient starvation-responsive lncRNA,[16] which is generated from the antisense strand of histone demethylase JHDM1D. Several studies have indicated that JHDM1D functions as a tumor suppressor in multiple cancer types, including prostate cancer and cervical cancer.[17,18] In contrast to JHDM1D, lncRNA JHDM1D-AS1 plays an oncogenic role. It has been documented

Received 22 April 2019; accepted 21 September 2019;
https://doi.org/10.1016/j.omtn.2019.09.028.

Correspondence: Meiyan Feng, Department of Pathology, Harbin Medical University Cancer Hospital, 150 Haping Road, Harbin, China.
E-mail: meiy_feng@163.com
Correspondence: Kuan Wang, Department of Gastrointestinal Surgery, Harbin Medical University Cancer Hospital, Harbin, China.
E-mail: 88008008@sina.com

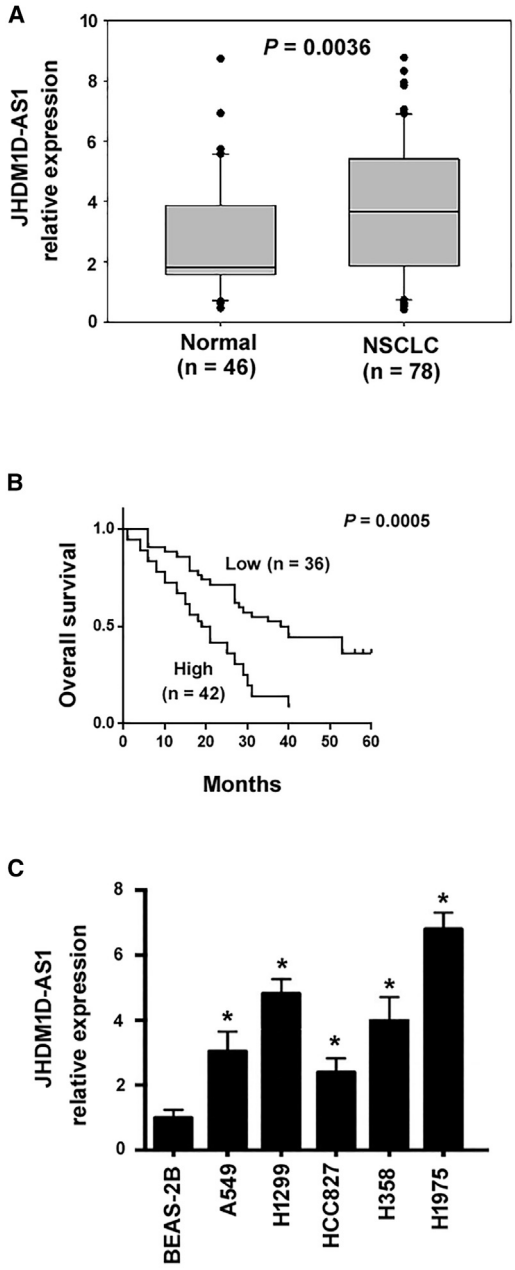

Figure 1. JHDM1D-AS1 Is Upregulated in NSCLC and Predicts Poor Prognosis

(A) Expression of JHDM1D-AS1 in 78 NSCLC and 46 adjacent normal lung tissues. (B) Kaplan-Meier analysis of overall survival in NSCLC patients according to JHDM1D-AS1 expression. (C) Expression levels of JHDM1D-AS1 in NSCLC and BEAS-2B bronchial epithelial cell lines. *p < 0.05 versus BEAS-2B cells.

that JHDM1D-AS1 promotes tumor growth in pancreatic cancer by inducing the expression of angiogenic factors.[16] Most interestingly, the JHDM1D-AS1 target gene signature has been proposed as a prognostic factor for lung cancer,[16] implying an association between JHDM1D-AS1 and lung cancer progression. However, the expression and function of JHDM1D-AS1 in NSCLC remain largely unknown.

Table 1. Correlation Between JHDM1D-AS1 Expression and Clinicopathological Features of NSCLC Patients (n = 78)

		JHDM1D-AS1		
Variable	N	Low Expression (n = 36)	High Expression (n = 42)	p Value
Age (years)				
<65	33	14	19	0.572
≥65	45	22	23	
Sex				
Male	51	21	30	0.226
Female	27	15	12	
TNM Stage				
I–II	28	19	9	0.004
III–IV	50	17	33	
T Classification				
T1–T2	35	20	15	0.0790
T3–T4	43	16	27	
Lymph Node Metastasis				
Negative	29	22	7	<0.001
Positive	49	14	35	

Here, we investigate the expression and prognostic significance of JHDM1D-AS1 in NSCLC. The effects of JHDM1D-AS1 knockdown or overexpression on the aggressive phenotype of NSCLC cells were determined. The mechanism mediating the action of JHDM1D-AS1 in NSCLC was further clarified.

RESULTS

JHDM1D-AS1 Is Upregulated in NSCLC and Predicts Poor Prognosis

In this work, we evaluated the prognostic significance of JHDM1D-AS1 in a cohort of 78 patients with NSCLC. The expression level of JHDM1D-AS1 was significantly greater in NSCLC specimens than that in adjacent normal lung tissues ($p = 0.0036$; Figure 1A). The NSCLC samples were divided into two groups depending on the JHDM1D-AS1 expression level. As shown in Table 1, high JHDM1D-AS1 expression was significantly correlated with advanced tumor, node, and metastasis (TNM) stage ($p = 0.004$) and lymph node metastasis ($p < 0.001$). Kaplan-Meier analysis showed that patients with high levels of tumoral JHDM1D-AS1 had a significantly shorter overall survival than did those with low levels ($p = 0.0005$; Figure 1B). Multivariate Cox regression analysis revealed JHDM1D-AS1 expression as an independent prognostic factor for overall survival of patients with NSCLC (Table 2). In addition, multiple NSCLC cell lines had an increased level of JHDM1D-AS1 compared to BEAS-2B bronchial epithelial cell lines ($p < 0.05$; Figure 1C). These results indicate that JHDM1D-AS1 overexpression has a poor prognostic impact on NSCLC.

Table 2. Univariate and Multivariate Cox Regression Analysis of Variables Associated with Overall Survival of NSCLC Patients

	Univariate		Multivariate	
Variable	HR (95% CI)	p Value	HR (95% CI)	p Value
Age, years (<65/≥65)	1.05 (0.61–1.72)	0.942	–	–
Sex (female/male)	1.48 (0.83–2.67)	0.235	–	–
TNM stage (I–II/III–IV)	1.82 (1.19–2.85)	0.009	1.66 (1.16–2.27)	0.015
T classification (T1–T2/T3–T4)	1.36 (0.67–2.27)	0.463	–	–
LN metastasis (negative/positive)	2.04 (1.20–3.14)	0.003	1.93 (1.14–3.02)	0.008
JHDM1D-AS1 (low/high)	2.29 (1.45–4.05)	<0.001	2.12 (1.33–3.26)	0.002

CI, confidence interval; HR, hazard ratio; LN, lymph node.

JHDM1D-AS1 Knockdown Suppresses the Aggressive Phenotype of NSCLC Cells

Next, we addressed whether JHDM1D-AS1 is required for the aggressive phenotype of NSCLC. To this end, we performed JHDM1D-AS1 knockdown studies using short hairpin RNA (shRNA) technology in both A549 and H1299 cells. The knockdown efficiency was validated by quantitative real-time PCR analysis (Figure 2A). Depletion of JHDM1D-AS1 significantly reduced the proliferative (Figure 2B) and invasive (Figure 2C) ability of NSCLC cells *in vitro*. Consistently, tumor growth (Figure 2D) and weight (Figure 2E) in the JHDM1D-AS1 knockdown group were significantly decreased compared with the control group. Bioluminescent imaging revealed that the development of lung metastasis was markedly suppressed by JHDM1D-AS1 deficiency (Figure 2F). To exclude the possibility of shRNA off-target effects, JHDM1D-AS1 rescue experiments were conducted. Of note, ectopic expression of JHDM1D-AS1 effectively restored the aggressive phenotype in NSCLC cells transfected with JHDM1D-AS1-targeting shRNA (Figure 2). Taken together, JHDM1D-AS1 plays an essential role in NSCLC growth and metastasis.

JHDM1D-AS1 Associates with DHX15 Protein in NSCLC Cells

To determine the mechanism underlying JHDM1D-AS1-mediated aggressive phenotype, we performed RNA pulldown assays followed by mass spectrometry using A549 cell lysates. As a result, we identified 25 JHDM1D-AS1-associated proteins. We chose five cancer-related proteins for further validation, i.e., BCLAF1, HSP90AB1, DHX15, PKM2, and XRCC5 (Table S1). Interestingly, we validated the presence of DHX15 in the complex pulled down by JHDM1D-AS1 in H1299 cells (Figure 3A). However, the other four candidates were not detected in the JHDM1D-AS1 pulldown (data not shown). A RNA immunoprecipitation (RIP) assay confirmed that JHDM1D-AS1 was enriched in DHX15 immunoprecipitates from A549 and H1299 cells (Figure 3B). In addition, JHDM1D-AS1 and DHX15 were co-localized in the nucleus of NSCLC cells (Figure 3C). Among the DHX15-positive cells, 60%–80% showed the co-localization with JHDM1D-AS1. These results suggest JHDM1D-AS1 binding to DHX15 protein.

Next, we tested whether JHDM1D-AS1 affects the expression of DHX15 protein. We demonstrated that knockdown of JHDM1D-AS1 led to a reduction in DHX15 protein levels in NSCLC cells (Figure 3D). When protein synthesis was inhibited by cycloheximide (CHX), DHX15 protein was significantly less stable in JHDM1D-AS1-deficient NSCLC cells relative to control cells (Figure 3E). The reduction of DHX15 in JHDM1D-AS1-depleted cells was markedly rescued by treatment with MG132, a proteasome inhibitor (Figure 3F). Taken together, these data indicate that JHDM1D-AS1 knockdown reduces DHX15 protein levels in NSCLC cells through proteasome-mediated degradation.

DHX15 Acts as an Oncogene in NSCLC Cells

We also performed immunohistochemistry of DHX15 on the same cohort of patients as used in the assay for JHDM1D-AS1. As shown in Figures 4A and 4B, the rate of DHX15-positive expression was significantly higher in NSCLC tissues (44.9%, 35/78) than that in adjacent normal lung tissues (15.4%, 12/78; $p = 0.0012$). Next, we explored the biological function of DHX15 in NSCLC cells. We performed DHX15 overexpression experiments in A549 cells (Figure 4C). As a consequence, NSCLC cells with DHX15 overexpression showed an increase in proliferation (Figure 4D) and invasion (Figure 4E). Furthermore, *in vivo* experiments revealed that DHX15 overexpression significantly augmented the growth of NSCLC xenograft tumors (Figures 4F and 4G). To complement the overexpression studies, shRNA-based knockdown of DHX15 was carried out. Transfection with DHX15-targeting shRNAs effectively reduced DHX15 expression in A549 cells compared with nonspecific negative controls (Figure 4C). Knockdown of DHX15 resulted in a decrease in A549 cell proliferation (Figure 4D), invasion (Figure 4E), and tumorigenesis (Figures 4F and 4G). These results indicate that DHX15 favors the growth and invasion of NSCLC cells.

DHX15 Mediates JHDM1D-AS1-Induced Aggressiveness in NSCLC Cells

Next, we investigated the function of DHX15 in mediating JHDM1D-AS1 effects on NSCLC cells. We showed that JHDM1D-AS1-induced NSCLC cell proliferation (Figure 5A) and invasion (Figure 5B) were impaired when DHX15 was silenced. These results suggest that the JHDM1D-AS1-dependent aggressive phenotype in NSCLC is mediated, at least in part, through regulation of DHX15 protein levels.

In addition, we examined whether overexpression of DHX15 could rescue the defects in cancer cell proliferation and invasion caused by JHDM1D-AS1 depletion. As shown in Figure 5C, overexpression of DHX15 attenuated the suppressive effect of JHDM1D-AS1 knockdown on NSCLC cell proliferation. Moreover, the invasiveness of JHDM1D-AS1-depleted NSCLC cells was promoted by DHX15 overexpression (Figure 5D).

DISCUSSION

Based on the Affymetrix Exon array data from an institutional database RefExA (http://www.lsbm.org/site_e/database/index.html), Kondo et al.[16] found that JHDM1D-AS1 is highly expressed in

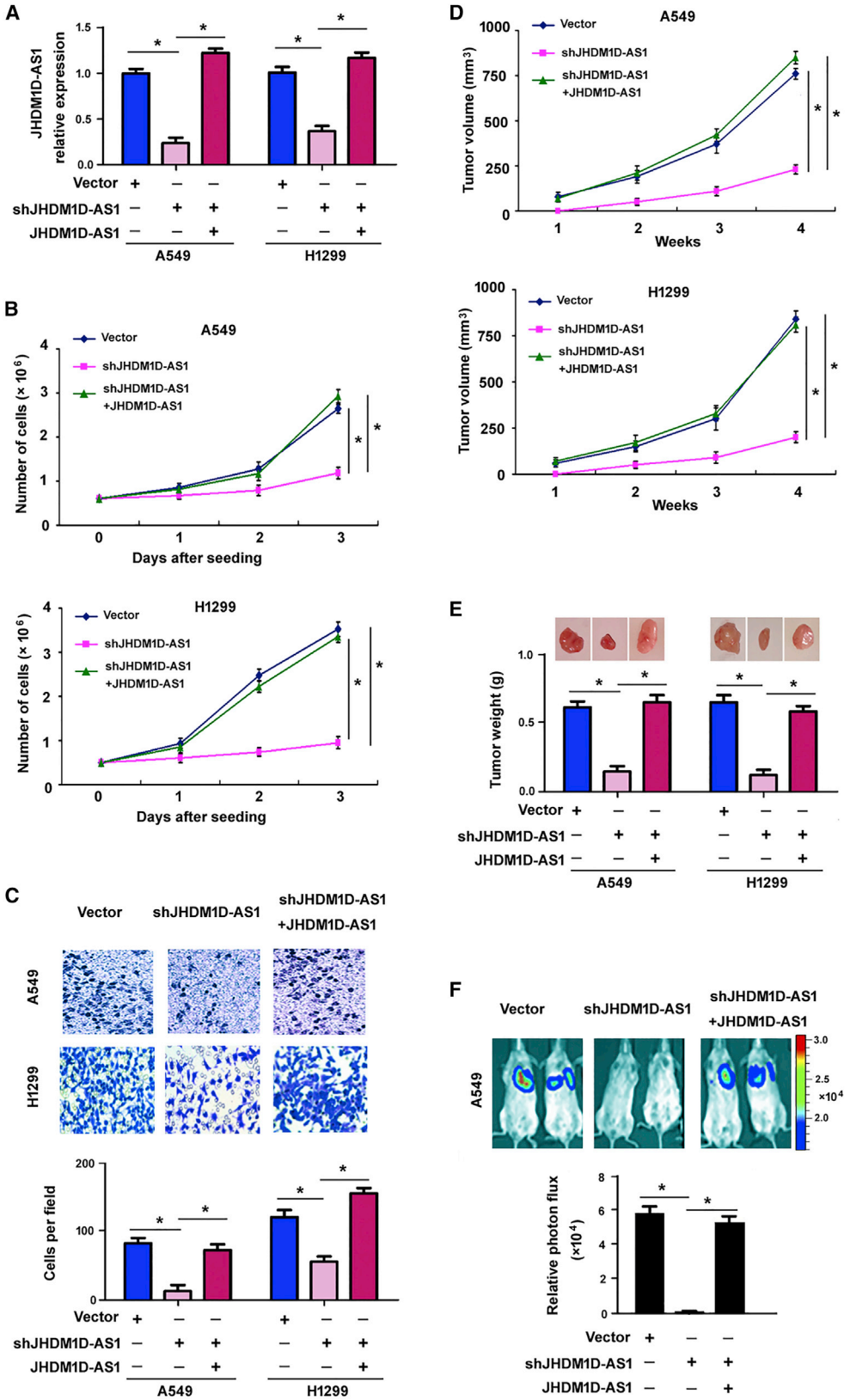

(legend on next page)

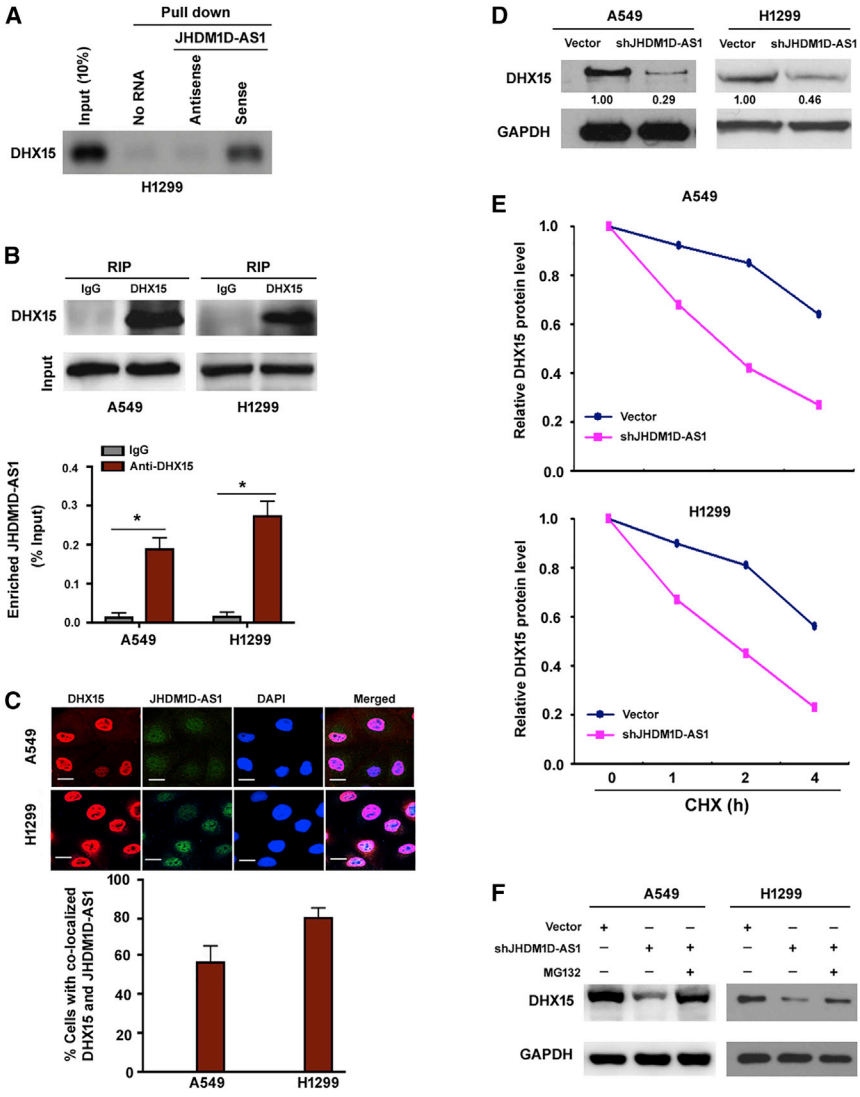

Figure 3. JHDM1D-AS1 Associates with DHX15 Protein in NSCLC Cells

(A) RNA pull-down assay showing that DHX15 protein is pulled down by JHDM1D-AS1 sense transcripts. (B) DHX15 RIP assay showing that JHDM1D-AS1 is enriched in DHX15 immunoprecipitates from A549 and H1299 cells. *$p < 0.05$. (C) Co-localization of JHDM1D-AS1 and DHX15 in NSCLC cells. JHDM1D-AS1 was detected by FITC-labeled probes using fluorescence *in situ* hybridization. Cells were also subjected to immunofluorescence staining with anti-DHX15 antibody. Scale bars, 10 μm. The percentage of the cells with co-localized JHDM1D-AS1 and DHX15 out of DHX15-positive cells was determined. (D) A549 and H1299 cells were transfected with JHDM1D-AS1-targeting shRNA and then subjected to western blot analysis to examine DHX15 expression. (E) A549 and H1299 cells transfected with JHDM1D-AS1-targeting shRNA were treated with CHX and tested for DHX15 protein levels at different time points. (F) Western blot analysis of DHX15 protein in NSCLC cells transfected with indicated constructs and treated for 5 h with or without 10 μM MG132.

multiple cancer types, including gastric cancer, lung cancer, breast cancer, ovarian cancer, renal cancer, and testicular cancer. Congruently, our data show that JHDM1D-AS1 expression is increased in NSCLC relative to adjacent normal lung tissues. We also demonstrate that high JHDM1D-AS1 expression is significantly correlated with advanced TNM stage and lymph node metastasis in NSCLC patients. Moreover, high levels of JHDM1D-AS1 result in poor overall survival. Multivariate Cox regression analysis points toward JHDM1D-AS1 as an independent prognostic marker. These results suggest that JHDM1D-AS1 plays an important role in NSCLC progression.

JHDM1D-AS1 has been reported to sense nutrient insufficiency and initiate tumor angiogenesis in pancreatic cancer,[16] but its role in NSCLC is unclear. Our present data provide evidence that JHDM1D-AS1 is required for the aggressiveness of NSCLC. We demonstrate that knockdown of JHDM1D-AS1 leads to diminished proliferation and invasion of NSCLC cells. The *in vivo* studies recapitulate the *in vitro* observations and show that JHDM1D-AS1 deficiency ablates tumor growth and metastasis in xenograft models. The proliferative and invasive defects of JHDM1D-AS1-depleted NSCLC cells were reversed by ectopic expression of JHDM1D-AS1. These results unveil an oncogenic role for JHDM1D-AS1 in NSCLC, and they provide an explanation for the worse prognosis in NSCLC with high JHDM1D-AS1 expression.

It has been documented that lncRNAs can exert their biological activities through interaction with protein partners.[19,20] For instance, the

Figure 2. JHDM1D-AS1 Knockdown Suppresses the Aggressive Phenotype of NSCLC Cells

(A) Measurement of JHDM1D-AS1 expression in A549 and H1299 cells transfected with indicated constructs. (B) A549 and H1299 cells transfected with indicated constructs were cultured for 3 days, and cell proliferation was determined by direct cell counting. (C) The invasion ability of A549 and H1299 cells transfected with indicated constructs was assessed by a Transwell invasion assay. (D) Tumor volumes of A549 and H1299 xenograft tumors were measured at different weeks after cell injection (n = 4). (E) Tumor weight was determined at the endpoint (n = 4). Representative images of xenograft tumors are shown. (F) *In vivo* metastasis assay. Luciferase-labeled A549 cells were injected via the tail vein at 4×10^6 cells per mouse. Representative bioluminescence images were taken at 5 weeks after cell injection. Bar graphs showing quantification of bioluminescence intensities (n = 4). *$p < 0.05$.

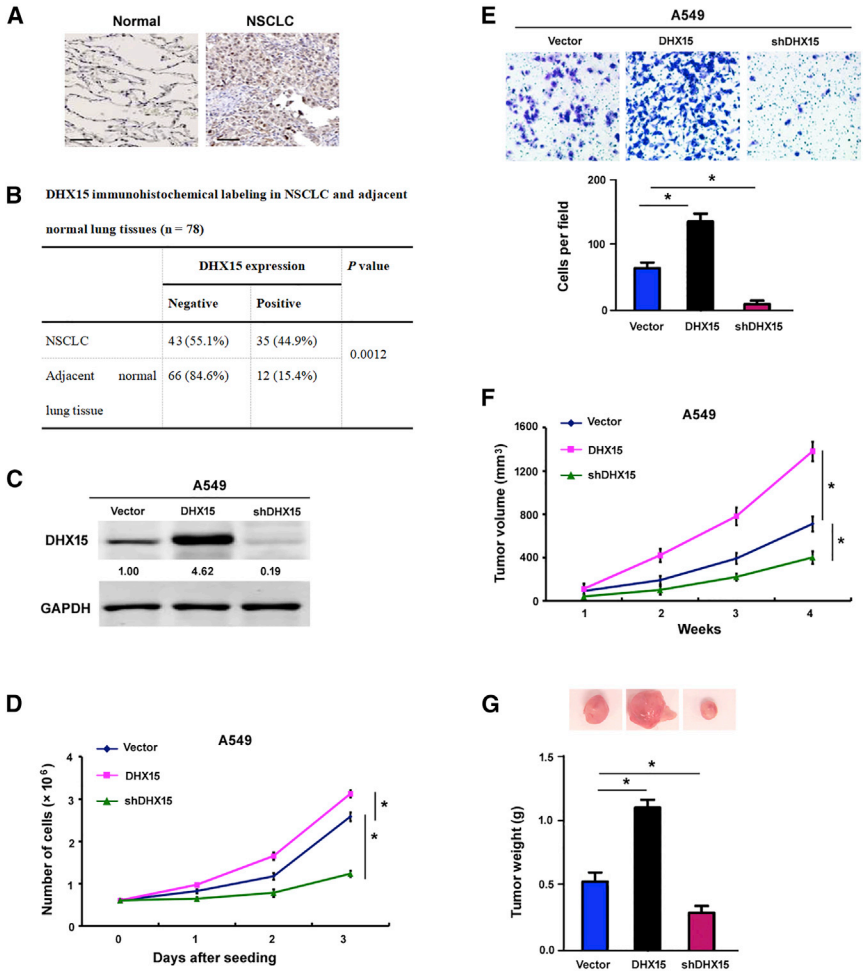

Figure 4. DHX15 Acts as an Oncogene in NSCLC Cells

(A) Representative immunohistochemical data for DHX15 expression in NSCLC and its adjacent normal tissue. Scale bar, 100 μm. (B) Evaluation of DHX15 immunohistochemical staining in 78 pairs of NSCLC and adjacent normal tissues. (C) DHX15 protein levels were detected by western blot analysis in A549 cells transfected with indicated constructs. (D) Cell proliferation determined by direct cell counting. (E) The invasion ability of A549 cells was assessed by a Transwell invasion assay. (F) Tumor volumes of A549 xenograft tumors were measured at different weeks after cell injection (n = 4). (G) Tumor weight was determined at the endpoint (n = 4). Representative images of xenograft tumors are shown. *p < 0.05.

lncRNA GLS-AS suppresses the expression of Myc by destabilizing Myc protein, and in turn attenuates the growth and invasion of pancreatic cancer cells.[19] The lncRNA LINC00707 was found to enhance gastric cancer metastasis by interacting with HuR, a mRNA stabilizing protein.[20] To identify JHDM1D-AS1-associated proteins, we performed RNA pull-down followed by mass spectrometry. Noticeably, we found that JHDM1D-AS1 associates with DHX15 protein in NSCLC cells. Furthermore, knockdown of JHDM1D-AS1 decreases the protein level of DHX15, which is ascribed to reduced protein stability. Treatment with the proteasome inhibitor MG132 blocks the reduction of DHX15 protein in JHDM1D-AS1-depleted cells. These observations indicate that JHDM1D-AS1 binding attenuates proteasome-mediated degradation of DHX15. Future work needs to map the domains of interactions between JHDM1D-AS1 and DHX15.

As a member of the RNA helicase family, DHX15 has RNA unwinding activity and participates in pre-rRNA processing.[7] A previous study reported that the G-quadruplex structure mediates the interaction between lncRNA GSEC and DHX36, suggesting a sequence structure-dependent DHX protein binding to lncRNAs.[21] This study provides an explanation for our findings that the sense (but not antisense) strand of JHDM1D-AS1 can bind to DHX15 protein. Ongoing studies are seeking to determine the essential JHDM1D-AS1 sequence mediating the direct interaction with DHX15.

DHX15 is known as an ATP-dependent RNA helicase involved in the antiviral response and ribosome biogenesis.[6,7] DHX15 is dysregulated in several types of cancers such as glioma, prostate cancer, and hepatocellular carcinoma.[9–11] The function of DHX15 in tumor progression depends on the cellular context. In particular, DHX15 acts as a tumor suppressor in glioma,[9] but as an oncogene in prostate cancer.[11] Although the role of DHX15 in NSCLC is still elusive, several other members of the DEXD/H box helicase family have been shown to participate in NSCLC progression. For instance, DDX5 was found to induce NSCLC tumorigenesis through β-catenin signaling.[22] Another example is that DDX17 contributes to the acquisition of gefitinib resistance in NSCLC cells.[23] Our data show that DHX15 overexpression promotes the proliferation, invasion, and tumorigenesis of NSCLC cells, whereas depletion of DHX15 restrains NSCLC cell proliferation and invasion. Clinically, DHX15 expression is elevated in NSCLC compared to adjacent normal lung tissues. Taken together, we provide the first evidence that DHX15 acts as an oncogene in NSCLC.

2Given the interaction between DHX15 protein and JHDM1D-AS1, we propose a possibility that DHX15 may mediate the oncogenic activity of JHDM1D-AS1 in NSCLC. In support of this possibility, we show that DHX15 knockdown impairs the JHDM1D-AS1-mediated aggressive phenotype of NSCLC cells. Moreover, overexpression of DHX15 rescues the effects of JHDM1D-AS1 silencing on NSCLC cell proliferation and invasion. Therefore, JHDM1D-AS1-mediated aggressiveness depends on the expression of DHX15.

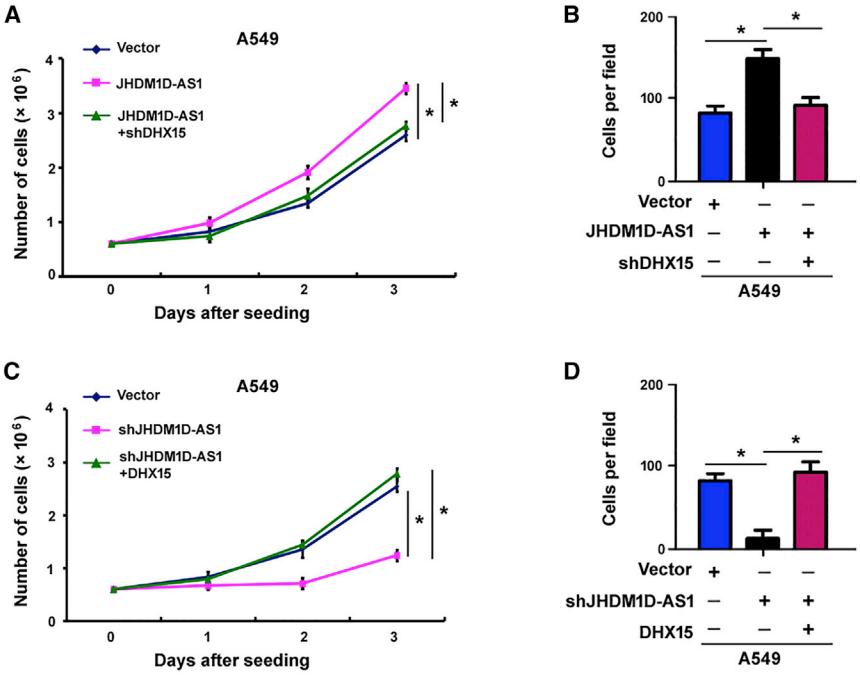

Figure 5. DHX15 Mediates JHDM1D-AS1-Induced Aggressiveness in NSCLC Cells

(A and C) Cell proliferation was determined by direct cell counting in A549 cells transfected with the indicated constructs. (B and D) The invasion ability of A549 cells was assessed by a Transwell invasion assay. *p < 0.05.

Previous studies have suggested that some antisense lncRNAs can modulate the expression of neighboring genes.[24,25] For instance, Esposito et al.[24] reported that the antisense lncRNA COMET is positively correlated with MET expression in papillary thyroid carcinoma. Zhu et al.[25] reported that the lncRNA HAS2-AS1 can stabilize HAS2 protein, thus contributing to hypoxia-induced invasiveness in oral squamous cell carcinoma cells. JHDM1D-AS1 is known to arise from the antisense strand of JHDM1D, which plays an opposite role to JHDM1D-AS1 in tumor angiogenesis.[17] However, overexpression or knockdown of JHDM1D-AS1 does not affect the expression of JHDM1D in NSCLC cells (data not shown), suggesting that JHDM1D-AS1-induced aggressiveness involves a JHDM1D-independent mechanism.

In conclusion, we identify the JHDM1D-AS1/DHX15 axis as a key driver of NSCLC metastasis. JHDM1D-AS1 binding stabilizes DHX15, consequently accelerating tumor cell proliferation and invasion. In addition, JHDM1D-AS1 overexpression is an independent prognostic factor for overall survival of patients with NSCLC. Our results offer potential novel targets for the treatment of NSCLC.

MATERIALS AND METHODS

Patients and Tissue Specimens

A total of 78 tumor samples and 46 adjacent normal tissues were collected from patients with NSCLC who underwent surgical resection at Harbin Medical University Cancer Hospital (Harbin, China). Clinicopathological information was retrieved from patient medical records. No patient received any anticancer treatment before surgery. Surgical specimens were immediately frozen in liquid nitrogen and stored at −80°C until RNA analysis. Written informed consent was obtained from each patient. The collection and application of patient specimens were approved by the Human Ethics Committee of Harbin Medical University Cancer Hospital.

Cell Lines

Human NSCLC cell lines (A549, H1299, HCC827, H358, and H1975) as well as BEAS-2B bronchial epithelial cells were purchased from the Cell Bank of Shanghai Institute of Cell Biology, Chinese Academy of Sciences (Shanghai, China). NSCLC cell lines were cultured in RPMI 1640 medium supplemented with 10% fetal bovine serum (FBS; Invitrogen, Grand Island, NY, USA); BEAS-2B cells were cultured in growth factor-supplemented medium (BEGM; Lonza, Walkersville, MD, USA). All cell lines were maintained in a humidified atmosphere of 5% CO_2 at 37°C.

RNA Isolation and Quantitative Real-Time PCR Analysis

Total RNA was extracted from tissue samples and cell lines using the PureLink RNA mini kit (Thermo Fisher Scientific, Waltham, MA, USA). RNA samples were reverse transcribed into cDNA using the SuperScript III reverse transcriptase kit (Invitrogen). The quantitative real-time PCR assay was performed using the SYBR Green RT-PCR kit (Takara Biotechnology, Dalian, China), according to the manufacturer's protocols. The PCR primers are as follows: JHDM1D-AS1: forward, 5′-CCTCGCGACGCTGAGAGAATC-3′ and reverse, 5′-ACGGCACATTCCTCCCTCGGA-3′; GAPDH: forward, 5′-ACCACAGTCCATGCCATCAC-3′ and reverse, 5′-TCCACCCTGTTGCTGTA-3′. The relative expression of JHDM1D-AS1 was normalized to GAPDH and analyzed by the $2^{-\Delta\Delta CT}$ method.[26]

Plasmids

For gene overexpression experiments, full-length human JHDM1D-AS1 and DHX15 were amplified by PCR and cloned to pcDNA3.1+ vector. For knockdown experiments, JHDM1D-AS1- and DHX15-targeting shRNA were commercially synthesized and cloned to the pLKO.1 vector.

Cell Transfection

Cell transfection was performed using Lipofectamine 3000 (Invitrogen), following the manufacturer's protocol. To generate stable cell

lines, transfected cells were selected with G418 (600 μg/mL) or puromycin (1 μg/mL; Sigma-Aldrich, St. Louis, MO, USA). In some experiments, transfected cells were treated with MG132 (10 μM; Sigma-Aldrich) for 5 h before analysis of DHX15 protein levels.

Cell Proliferation Assay

Cells were seeded into 12-well plates (4 or 6 × 10^5 cells/well) and allowed to grow for 3 days. Cells were counted every day, and growth curves were plotted.

Transwell Invasion Assay

A Transwell invasion assay was performed as described previously.[27] Transwell chambers (8-μm pore size) in a 24-well plate were used this assay. 1 × 10^5 cells suspended in RPMI 1640 medium without FBS were seeded into the upper insert, while the lower insert was filled with fresh complete medium containing 10% FBS. After a 48-h incubation, invading cells were fixed, stained with crystal violet, and counted.

Animal Experiments

All animal experiments were conducted in accordance with national and international guidelines and approved by the Animal Care and Use Institutional Review Board of Harbin Medical University Cancer Hospital. Six-week-old male BALB/c nude mice were housed in specific pathogen-free conditions on a 12-h light/12-h dark cycle with free access to food and water. Stably transfected A549 and H1299 cells were subcutaneously injected into nude mice (3 × 10^6 cells/mouse). Tumor size was recorded every week using a caliper. Tumor volumes were calculated based on the following formula: Volume = ($L \times W^2$)/2, with L being the largest diameter (mm) and W being the smallest diameter (mm). Animals were sacrificed after 4 weeks, and tumor weights were recorded. For the *in vivo* metastasis assay, A549 cells were co-transfected with JHDM1D-AS1-targeting shRNA, JHDM1D-AS1-expressing plasmid, as well as luciferase-expressing vector and injected via the tail vein at 4 × 10^6 cells per mouse. Noninvasive bioluminescence imaging was conducted to monitor tumor metastasis. Each group had four mice.

RNA Pull-Down Assay

The RNA pull-down assay was conducted as described previously.[28] Briefly, biotin-labeled JHDM1D-AS1 (sense or antisense) was obtained with Biotin RNA Labeling Mix and T7 RNA polymerase (Roche Diagnostics, Indianapolis, IN, USA) and purified with the RNeasy Mini Kit (QIAGEN, Valencia, CA, USA). The resultant biotinylated RNA was incubated with the lysate from H1299 cells at 4°C overnight, followed by incubation with streptavidin magnetic beads (Invitrogen) for 1 h at room temperature. The proteins pulled down were subjected to western blot analysis for DHX15.

RIP Assay

A RIP assay was done as described previously.[29] Briefly, A549 and H1299 cells were lysed in RIP buffer containing protease/RNase inhibitors (Sigma-Aldrich). The lysate was incubated with anti-IgG (negative control) or anti-DHX15 antibody (Thermo Fisher Scientific, Waltham, MA, USA) conjugated with protein A/G magnetic beads. The immunoprecipitates were treated with Proteinase K, and the immunoprecipitated RNA was detected by quantitative real-time PCR analysis.

Western Blot Analysis

Cells were lysated in radioimmunoprecipitation assay lysis buffer supplemented with a protease inhibitor cocktail (Sigma-Aldrich). Protein samples were separated on SDS-PAGE and transferred to polyvinylidene difluoride membranes. The membranes were blocked with 5% fat-free milk at room temperature for 1 h, followed by overnight incubation at 4°C with primary antibodies anti-DHX15 and anti-GAPDH (Thermo Fisher Scientific). The membranes were then incubated with secondary antibodies (Cell Signaling Technology, Waltham, MA, USA). Signals were visualized using the Pierce enhanced chemiluminescence (ECL) western blotting substrate (Thermo Fisher Scientific).

Fluorescence *In Situ* Hybridization and Immunofluorescence Staining

JHDM1D-AS1 probe was labeled with fluorescein isothiocyanate (FITC) using Agilent's Quick Amp Labeling Kit (Agilent Technologies, Santa Clara, CA, USA). Cells were fixed in 4% formaldehyde, permeabilized with 0.5% Triton X-100, and hybridized with FITC-labeled JHDM1D-AS1 probe. Cells were also subjected to immunofluorescence staining with anti-DHX15 antibody (Thermo Fisher Scientific) and Alexa Fluor 594 goat anti-rabbit IgG (Thermo Fisher Scientific). Nuclei were stained with DAPI. Colocalization images were obtained under a confocal microscope.

CHX Chase Assay

A CHX chase assay was conducted as described previously.[30] Briefly, JHDM1D-AS1-depleted and control cells were treated with CHX (100 μg/mL; Sigma-Aldrich) for 0, 1, 2, and 4 h. The cells were harvested and tested for the turnover of DHX15 protein by western blot analysis.

Immunohistochemistry

Formalin-fixed and paraffin-embedded specimens were deparaffinized, rehydrated, and treated for antigen retrieval using sodium citrate buffer. After blocking endogenous peroxidase in 3% H_2O_2, the sections were incubated with primary antibody to DHX15 (1:100 dilution; Thermo Fisher Scientific) overnight at 4°C, followed by incubation with horseradish peroxidase-conjugated anti-rabbit IgG. Chromogen development was performed using a diaminobenzidine (DAB) chromogenic substrate kit. The sections were then counterstained with hematoxylin.

For evaluation of immunohistochemical results, the intensity of staining was scored as follows: 0 (no staining), 1 (weak), 2 (moderate), and 3 (high). The percentage of immunolabeling was categorized into four groups: 1 (1%–15%), 2 (16%–30%), 3 (31%–70%), and 4 (71%–100%). The product of the staining intensity multiplied by the percentage of immunolabeling was determined for each tumor sample. The samples

with the final score of ≥4 were considered to have positive expression.

Statistical Analysis

Data are presented as the mean ± SD and analyzed by the Student's t test or one-way ANOVA with a Tukey *post hoc* test. The difference in JHDM1D-AS1 expression between NSCLC and adjacent normal tissues was determined using the Mann-Whitney U test. The chi-square test was used to analyze the relationship between JHDM1D-AS1 expression and clinicopathologic parameters of NSCLC. Survival curves were plotted using the Kaplan-Meier method and compared using the log-rank test. The univariate and multivariate Cox proportional hazards models were used to determine the prognostic significance of risk factors. A value of $p < 0.05$ was considered statistically significant.

SUPPLEMENTAL INFORMATION

Supplemental Information can be found online at https://doi.org/10.1016/j.omtn.2019.09.028.

AUTHOR CONTRIBUTIONS

G.Y., M.F., and K.W. designed the experiments and analyzed data. Y.Q., K.C., and Y.N. performed the *in vitro* experiments. X.Z., S.X., and C.Z. performed the *in vivo* experiments. G.Y. and K.W. wrote the manuscript. All authors reviewed and approved the final manuscript.

CONFLICTS OF INTEREST

The authors declare no competing interests.

ACKNOWLEDGMENTS

This work was supported by the Nn10 Program of Harbin Medical University Cancer Hospital of China (Nn10 PY2017-04) and Haiyan Research Foundation of Harbin Medical University Cancer Hospital of China (JJZD2016-02).

REFERENCES

1. Siegel, R.L., Miller, K.D., and Jemal, A. (2017). Cancer statistics, 2017. CA Cancer J. Clin. *67*, 7–30.

2. Hirsch, F.R., Scagliotti, G.V., Mulshine, J.L., Kwon, R., Curran, W.J., Jr., Wu, Y.L., and Paz-Ares, L. (2017). Lung cancer: current therapies and new targeted treatments. Lancet *389*, 299–311.

3. Chen, Z., Fillmore, C.M., Hammerman, P.S., Kim, C.F., and Wong, K.K. (2014). Non-small-cell lung cancers: a heterogeneous set of diseases. Nat. Rev. Cancer *14*, 535–546.

4. Fraile, J.M., Campos-Iglesias, D., Rodríguez, F., Astudillo, A., Vilarrasa-Blasi, R., Verdaguer-Dot, N., Prado, M.A., Paulo, J.A., Gygi, S.P., Martín-Subero, J.I., et al. (2018). Loss of the deubiquitinase USP36 destabilizes the RNA helicase DHX33 and causes preimplantation lethality in mice. J. Biol. Chem. *293*, 2183–2194.

5. Semlow, D.R., Blanco, M.R., Walter, N.G., and Staley, J.P. (2016). Spliceosomal DEAH-box ATPases remodel pre-mRNA to activate alternative splice sites. Cell *164*, 985–998.

6. Lu, H., Lu, N., Weng, L., Yuan, B., Liu, Y.J., and Zhang, Z. (2014). DHX15 senses double-stranded RNA in myeloid dendritic cells. J. Immunol. *193*, 1364–1372.

7. Memet, I., Doebele, C., Sloan, K.E., and Bohnsack, M.T. (2017). The G-patch protein NF-κB-repressing factor mediates the recruitment of the exonuclease XRN2 and activation of the RNA helicase DHX15 in human ribosome biogenesis. Nucleic Acids Res. *45*, 5359–5374.

8. Inesta-Vaquera, F., Chaugule, V.K., Galloway, A., Chandler, L., Rojas-Fernandez, A., Weidlich, S., Peggie, M., and Cowling, V.H. (2018). DHX15 regulates CMTR1-dependent gene expression and cell proliferation. Life Sci Alliance *1*, e201800092.

9. Ito, S., Koso, H., Sakamoto, K., and Watanabe, S. (2017). RNA helicase DHX15 acts as a tumour suppressor in glioma. Br. J. Cancer *117*, 1349–1359.

10. Jing, Y., Nguyen, M.M., Wang, D., Pascal, L.E., Guo, W., Xu, Y., Ai, J., Deng, F.M., Masoodi, K.Z., Yu, X., et al. (2018). DHX15 promotes prostate cancer progression by stimulating Siah2-mediated ubiquitination of androgen receptor. Oncogene *37*, 638–650.

11. Xie, C., Liao, H., Zhang, C., and Zhang, S. (2019). Overexpression and clinical relevance of the RNA helicase DHX15 in hepatocellular carcinoma. Hum. Pathol. *84*, 213–220.

12. Wang, F., Chainani, P., White, T., Yang, J., Liu, Y., and Soibam, B. (2018). Deep learning identifies genome-wide DNA binding sites of long noncoding RNAs. RNA Biol. *15*, 1468–1476.

13. Liu, B., Pan, S., Xiao, Y., Liu, Q., Xu, J., and Jia, L. (2018). LINC01296/miR-26a/GALNT3 axis contributes to colorectal cancer progression by regulating *O*-glycosylated MUC1 via PI3K/AKT pathway. J. Exp. Clin. Cancer Res. *37*, 316.

14. Wang, D., and Hu, Y. (2019). Long non-coding RNA PVT1 competitively binds microRNA-424-5p to regulate CARM1 in radiosensitivity of non-small-cell lung cancer. Mol. Ther. Nucleic Acids *16*, 130–140.

15. Xu, X., Lou, Y., Tang, J., Teng, Y., Zhang, Z., Yin, Y., Zhuo, H., and Tan, Z. (2019). The long non-coding RNA Linc-GALH promotes hepatocellular carcinoma metastasis via epigenetically regulating Gankyrin. Cell Death Dis. *10*, 86.

16. Kondo, A., Nonaka, A., Shimamura, T., Yamamoto, S., Yoshida, T., Kodama, T., Aburatani, H., and Osawa, T. (2017). Long noncoding RNA JHDM1D-AS1 promotes tumor growth by regulating angiogenesis in response to nutrient starvation. Mol. Cell. Biol. *37*, e00125-17.

17. Osawa, T., Muramatsu, M., Wang, F., Tsuchida, R., Kodama, T., Minami, T., and Shibuya, M. (2011). Increased expression of histone demethylase JHDM1D under nutrient starvation suppresses tumor growth via down-regulating angiogenesis. Proc. Natl. Acad. Sci. USA *108*, 20725–20729.

18. Lee, K.H., Hong, S., Kang, M., Jeong, C.W., Ku, J.H., Kim, H.H., and Kwak, C. (2018). Histone demethylase KDM7A controls androgen receptor activity and tumor growth in prostate cancer. Int. J. Cancer *143*, 2849–2861.

19. Deng, S.J., Chen, H.Y., Zeng, Z., Deng, S., Zhu, S., Ye, Z., He, C., Liu, M.L., Huang, K., Zhong, J.X., et al. (2019). Nutrient stress-dysregulated antisense lncRNA GLS-AS impairs GLS-mediated metabolism and represses pancreatic cancer progression. Cancer Res. *79*, 1398–1412.

20. Xie, M., Ma, T., Xue, J., Ma, H., Sun, M., Zhang, Z., Liu, M., Liu, Y., Ju, S., Wang, Z., and De, W. (2019). The long intergenic non-protein coding RNA 707 promotes proliferation and metastasis of gastric cancer by interacting with mRNA stabilizing protein HuR. Cancer Lett. *443*, 67–79.

21. Matsumura, K., Kawasaki, Y., Miyamoto, M., Kamoshida, Y., Nakamura, J., Negishi, L., Suda, S., and Akiyama, T. (2017). The novel G-quadruplex-containing long noncoding RNA GSEC antagonizes DHX36 and modulates colon cancer cell migration. Oncogene *36*, 1191–1199.

22. Wang, Z., Luo, Z., Zhou, L., Li, X., Jiang, T., and Fu, E. (2015). DDX5 promotes proliferation and tumorigenesis of non-small-cell lung cancer cells by activating β-catenin signaling pathway. Cancer Sci. *106*, 1303–1312.

23. Li, K., Mo, C., Gong, D., Chen, Y., Huang, Z., Li, Y., Zhang, J., Huang, L., Li, Y., Fuller-Pace, F.V., et al. (2017). DDX17 nucleocytoplasmic shuttling promotes acquired gefitinib resistance in non-small cell lung cancer cells via activation of β-catenin. Cancer Lett. *400*, 194–202.

24. Esposito, R., Esposito, D., Pallante, P., Fusco, A., Ciccodicola, A., and Costa, V. (2019). Oncogenic properties of the antisense lncRNA COMET in BRAF- and RET-driven papillary thyroid carcinomas. Cancer Res. *79*, 2124–2135.

25. Zhu, G., Wang, S., Chen, J., Wang, Z., Liang, X., Wang, X., Jiang, J., Lang, J., and Li, L. (2017). Long noncoding RNA HAS2-AS1 mediates hypoxia-induced invasiveness of oral squamous cell carcinoma. Mol. Carcinog. *56*, 2210–2222.

26. Livak, K.J., and Schmittgen, T.D. (2001). Analysis of relative gene expression data using real-time quantitative PCR and the $2^{-\Delta\Delta C(T)}$ method. Methods *25*, 402–408.

27. Dong, D., Mu, Z., Wei, N., Sun, M., Wang, W., Xin, N., Shao, Y., and Zhao, C. (2019). Long non-coding RNA ZFAS1 promotes proliferation and metastasis of clear cell renal cell carcinoma via targeting miR-10a/SKA1 pathway. Biomed. Pharmacother. *111*, 917–925.

28. Wang, F.W., Cao, C.H., Han, K., Zhao, Y.X., Cai, M.Y., Xiang, Z.C., Zhang, J.X., Chen, J.W., Zhong, L.P., Huang, Y., et al. (2019). APC-activated long noncoding RNA inhibits colorectal carcinoma pathogenesis through reduction of exosome production. J. Clin. Invest. *129*, 727–743.

29. Zhang, Y., Feng, Y., Hu, Z., Hu, X., Yuan, C.X., Fan, Y., and Zhang, L. (2016). Characterization of long noncoding RNA-associated proteins by RNA-immunoprecipitation. Methods Mol. Biol. *1402*, 19–26.

30. Xiong, Y., He, L., Shay, C., Lang, L., Loveless, J., Yu, J., Chemmalakuzhy, R., Jiang, H., Liu, M., and Teng, Y. (2019). Nck-associated protein 1 associates with HSP90 to drive metastasis in human non-small-cell lung cancer. J. Exp. Clin. Cancer Res. *38*, 122.